



Prospects for X-ray Studies of Galaxy Clusters with Astro-E2/XRS

T. Furusho¹, K. Mitsuda¹, N. Yamasaki¹, R. Fujimoto¹, and T. Ohashi²

¹ Institute of Space and Astronautical Science (ISAS), Japan Aerospace Exploration Agency (JAXA), 3-1-1 Yoshinodai, Sagamihara, Kanagawa 229-8510, Japan e-mail: furusho@astro.isas.jaxa.jp

² Department of Physics, Tokyo Metropolitan University, 1-1 Minamiohsawa, Hachioji, Tokyo 192-0397, Japan

Abstract. The Astro-E2 high resolution X-Ray Spectrometer (XRS) is expected to provide a major enhancement in study of clusters of galaxies. Astro-E2 is the fifth Japanese X-ray astronomy observatory, which is scheduled for launch in early 2005. The XRS instrument, developed under a Japan-US collaboration, is an X-ray microcalorimeter with a capability of observing extended objects, and a high energy resolution of about 6 eV at 6 keV. The spectral resolving power is 20 times higher than CCDs over the 0.5-10 keV energy band. We have obtained several new results of clusters with Chandra and XMM, which show that high-resolution imaging spectroscopy can clarify some outstanding questions. New sciences from Astro-E2 include the first clear measurement of gas velocities, determination of ion and electron temperatures, and electron densities based on the resolved line features. We will describe the XRS instrument design, and present simulations of the expected performance.

Key words. X-rays { Galaxy clusters

1. Introduction

Astro-E, the 5th Japanese X-ray astronomy satellite, was lost during the launch on February 10, 2000 due to a malfunction with the 1st stage of a M-V rocket. However, Astro-E was a very unique mission that carried the first X-ray microcalorimeter into space and would complement the great imaging performance of

Chandra and the large effective area of XMM-Newton. The rebuild mission Astro-E2 has been approved, and is scheduled for launch in early 2005.

Figure 1 shows a photograph of the Astro-E2 spacecraft under the first spacecraft integration test at ISAS/JAXA from July to November, 2003. The satellite has three instruments: an X-ray microcalorimeter (X-Ray Spectrometer; XRS), four X-ray CCD cameras (X-ray Imaging Spectrometer; XIS), and a scintillation counter with silicon PIN detectors

Send off print requests to: T. Furusho

Correspondence to: 3-1-1 Yoshinodai, Sagamihara, Kanagawa 229-8510, Japan

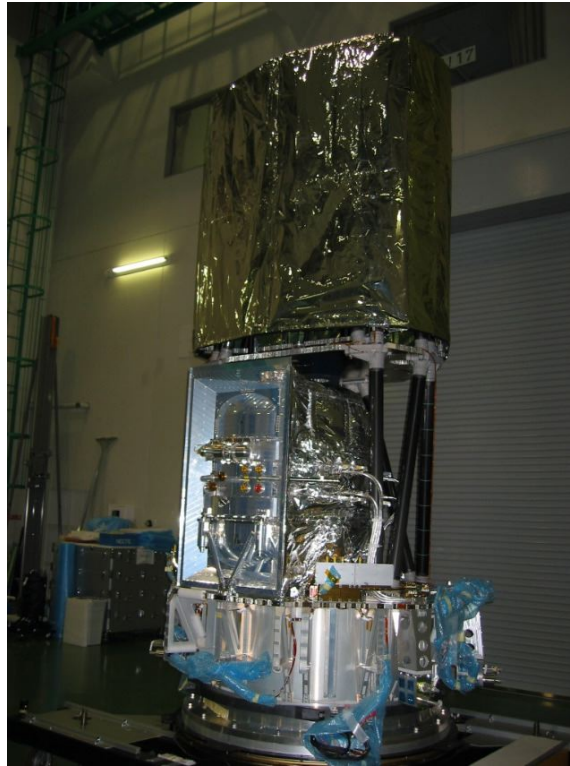


Fig. 1. The Astro-E2 satellite during the first spacecraft integration test at ISAS/JAXA. In this photograph, the spacecraft was not equipped with XRT or solar panels yet. The XRS Ne dewar sits at the spacecraft base plate.

(Hard X-ray Detector; HXD). XRS and XIS are put at each focal plane of five X-ray thin foil mirrors (X-Ray Telescope; XRT). They cover the soft energy band of 0.3–10 keV, while HXD extends the bandpass of the mission up to 700 keV. The spacecraft is approximately 1700 kg in weight, and about 6.5 m in length. The XRS dewar occupies a large volume with a weight of about 400 kg. A M-V rocket will bring the spacecraft into a circular near-earth orbit with a nominal altitude of 550 km, and an inclination of 31°. The detailed description of Astro-E2 and the progress are found at the web site: <http://www.astro.isas.jaxa.jp/astroe/index.html.en>.

2. X-ray spectrometer

XRS is the primary instrument of Astro-E2. The detector system was developed at NASA/Goddard Space Flight Center and University of Wisconsin. The baseline design of XRS for Astro-E2 is same as the original XRS onboard Astro-E. The detector system consists of 32 pixels with HgTe absorbers attached on silicon thermistors, operates at a temperature of 60 mK with solid Ne, liquid He, and an adiabatic demagnetization refrigerator to cool the detector down.

Once the Astro-E2 mission program was started, enormous efforts have been continued to make improvements based on our precious knowledge of the original XRS by practice. The XRS performance for both

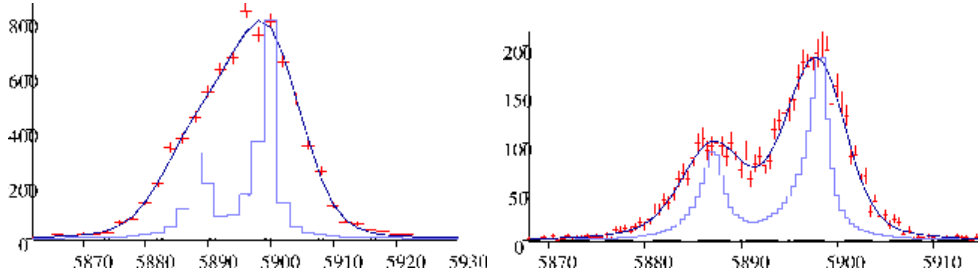


Fig. 2. Examples of Mn-K α spectra taken by the original bilinear array (left) and the new 2-dimensional array (right).

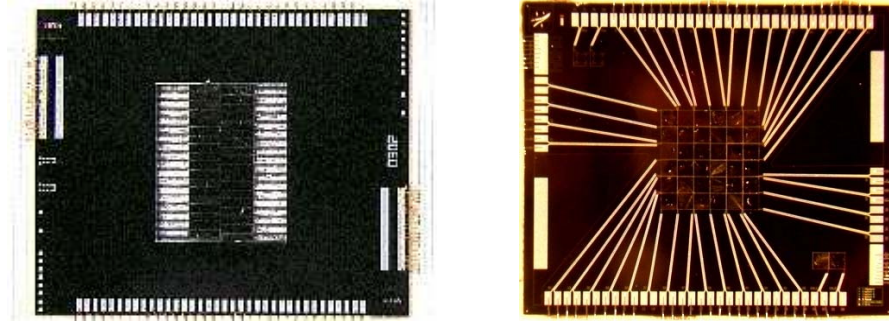


Fig. 3. The original 2 \times 16 bilinear array for Astro-E (left), and 6 \times 6 2-dimensional array for Astro-E2 (right).

Table 1. Performance of the original XRS of Astro-E and the new XRS of Astro-E2

	Astro-E	Astro-E2
Energy band	0.3{10 keV	0.3{10 keV
Energy resolution (FWHM at 6 keV)	12 eV	6 eV
Field of view	1.9 ^o 4.1 ^o	2.9 ^o 2.9 ^o
Array format	2 \times 16	6 \times 6
Number of pixels	32	31 + 1 (for calibration only)
Pixel size	1.23 \times 0.318 mm	0.624 \times 0.624 mm
Lifetime	< 2 years	2.5{3 years

Astro-E and Astro-E2 is summarized in Table 1. The following items are most remarkable improvements done for Astro-E2/XRS.

Higher energy resolution: Figure 2 shows examples of ^{55}Fe spectra (Mn-K lines) obtained from the original and new XRS (Stahle et al. 2002). The new XRS has an energy resolution of 6 eV at 6 keV ($E = E_0 = 1000$), a factor of 2 better than the original. The high spectral capability

enables us to resolve Mn-K α_1 and K α_2 lines beautifully, of which difference of the peak energies is 11 eV.

Longer lifetime: A major design change of the cooling system is an addition of a mechanical cooler outside the Ne dewar to improve a lifetime of XRS longer. The lifetime of the original XRS was limited to about 2 years by the amount of liquid He. With the mechanical cooler, the lifetime is expected to be at least 2.5 yr, or more.

Lower background: We also have changed a placement of in-flight calibration sources of ^{55}Fe and ^{41}Ca , which were originally attached inside the detector system that caused a significant background. The calibration sources will be attached to a filter wheel, which is located above the XRS outside the Ne dewar. Users can choose a filter with them, or without them. Instead of the internal calibration sources, we dedicate one of the 32 pixels for calibration only that is illuminated by a ^{55}Fe source. The design change of the calibration sources results in lower internal background and much higher sensitivity of the new XRS.

Better detector design: We adopt a 6×6 2-dimensional array covering $2.9^\circ \times 2.9^\circ$ field of view as shown in the right panel of Figure 3, instead of a 2×16 bilinear array as shown in the left panel. The 2-dimensional array is more suitable for observations of celestial objects as it results in lots of benefits of higher energy resolution, faster pulse response, etc.

Those improvements make XRS even more fascinating system. Now the right XRS array is under the ground calibration tests, and we will start the on-orbit spacecraft integration tests in April, 2004.

3. Feasibility study for science with galaxy clusters

Chandra and XMM-Newton have brought us new views with their ultimate imaging and spectroscopic capabilities. Astro-E2 is ongoing to join them to make a substantial contribution to science. The broad energy band-pass, spectroscopic resolving power covering up to 10 keV, and applicability to extended sources will provide a unique capability for dealing with fundamental problems in astrophysics. Galaxy clusters with a thermal spectrum of $kT = 3\text{--}10$ keV are the most suitable and interesting objects with XRS. We face on the new features such as lack of cool gas below 1 keV, complex cores together with radio lobes, various structures as a result of subcluster mergers, and

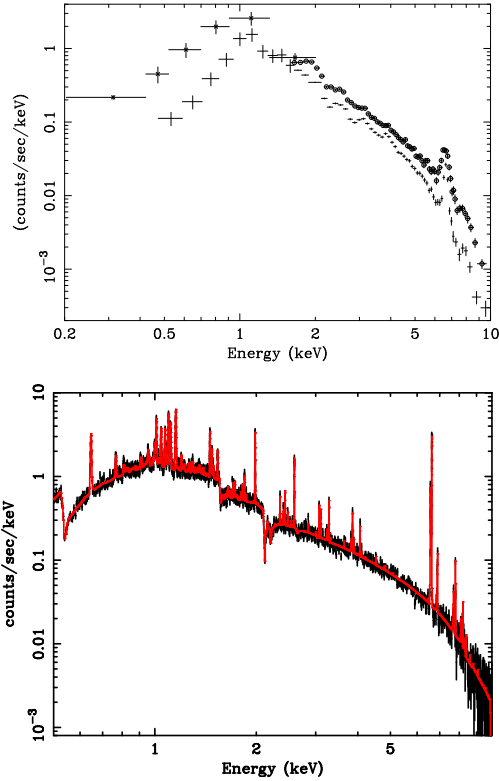


Fig. 4. Top panel: ASCA spectra of the Centaurus cluster. The upper spectrum with circles is of GIS, and the lower spectrum is of SIS. Bottom panel: A simulated XRS spectrum of the Centaurus cluster.

high metallicity rings. The XRS data will provide us a new, straightforward approach to solve those dynamical and thermal problems in clusters.

In this section, we give four examples of scientific topics in galaxy clusters based on XRS spectral simulations¹ to examine what kind of analysis we will be able to do. Needless to say, there are much more other interesting sciences that XRS possibly can do, for instance, thermal broadening, and soft emission excess using Oxygen lines.

¹ Responses used in this paper are prepared for the 4th Astro-E2 science working group meeting held in November, 2003

3.1. Abundances of various metals (line intensity)

First, we can divide complex lines into each single line so that we will determine the line intensity more precisely ever before. The top panel of Figure 4 shows spectra of the Centaurus cluster taken by SIS (CCD camera) and GIS (gas scintillation proportional counter) onboard ASCA (Ikebe et al. 1999). An apparent single line in the spectra is actually a blend of several lines, which we can not divide with a CCD's spectroscopic capability so far. However, we will finally resolve almost all lines of various metals in intercluster and intergalactic media. The bottom panel of Figure 4 is a simulated XRS spectrum of Centaurus, which shows a lot of sharp emission lines. We will measure absolute abundances of those lines from Oxygen to Nickel accurately and model-independently. We will also obtain a spatial distribution of each metal abundance even though it will be rough more than 30° step depending on the XRS pixel size and the XRT imaging capability.

3.2. Gas motion (line shift)

Second, we can determine line centers accurately, and detect line shifts using a Fe-K resonance line. The top panel of Figure 5 is a Chandra image of Abell 754, which is a famous merging cluster. ASCA and Chandra have shown that the cluster has a temperature structure and a density gap that indicate an ongoing strong merger in this cluster. The intracluster gas where this kind of large merger takes place expects that there is a gas bulk motion with a velocity of several hundred to 1000 km/s. The bottom panel shows simulated XRS spectra for two pointing observations shown as two green boxes in the top panel. We assume that an exposure time is 40 ks each, and a line-of-sight difference of the gas velocity is 500 km/s. The velocity difference, 10 eV at 6 keV, is easily detected as a shift of the line center. We can map out a velocity distribution in a direct way.

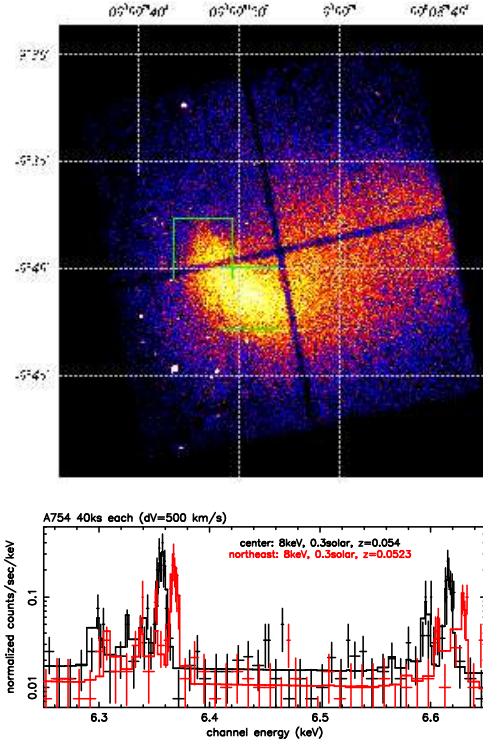


Fig. 5. Top panel: Chandra ACIS-I image of Abell 754. The two green boxes represent the XRS field of view. Bottom panel: Simulated XRS spectra of the two pointings overlaid on the image with 40 ks exposure each.

3.3. Turbulence (line broadening)

Third, we can look into an existence of line broadening that means a velocity dispersion by gas bulk motion. Recently, Sunyaev et al. (2003), and Inogamov & Sunyaev (2003) reported that a line broadening by hydrodynamic turbulences in the intergalactic gas could be present and detected in many clusters. Emission lines of heavy elements, especially of iron, are the most promising probes to measure turbulent velocities, because their thermal broadening is much smaller compared with that of protons. Figure 6 shows simulated XRS spectra for the complex of iron-K lines with an APEC model of $kT = 3$ keV with a velocity

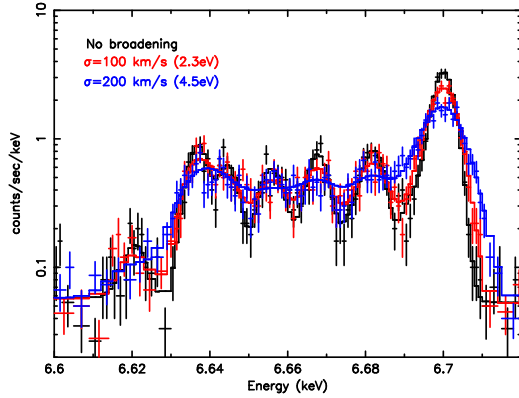


Fig. 6. Simulated spectra around Fe-K complex assuming with velocity dispersion by hydrodynamical turbulences of 0, 100, and 200 km/s (black, red, and blue, respectively).

dispersion of 100 and 200 km/s and no line broadening. If lines are broadened with a velocity of more than 200 km/s, they create a flat-topped line profile that are immediately distinguishable from a spiky profile with no line broadening.

3.4. Plasma diagnostics (line ratio)

Further, we can calculate line ratios of complex lines created by the structure. We can separate a resonance line (w) and intercombination (x,y) and forbidden (z) lines, and possibly other satellite lines (j,k,a etc.) as shown in Figure 7. Line ratios of those lines will enable us to do plasma diagnostics with Fe-K lines. Plasma diagnostics is expected to give us important physical parameters directly such as electron temperature, density, and ionization level. Note that the line ratios also are useful for direct analysis of resonance scattering in a dense cluster core such as of M87.

Now, we proceed the final tests of each subsystem including integration tests, calibration tests, performance tests, and environmental tests. The PV phase targets of Astro-E2 will be discussed soon and decided in March, 2004. First call for propos-

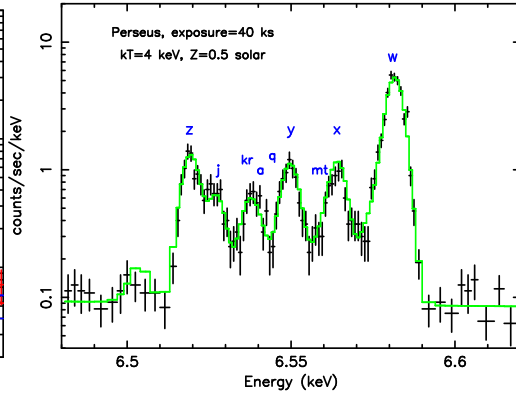


Fig. 7. Fe XXV lines with a 40 ks simulation of Perseus cluster.

als in the AO-1 phase, of which observations are starting six months later after the launch, will be announced in next spring, 2004.

Acknowledgements. We would like to thank R.L. Kelley, K.R. Boyce, C.A. Kilbourne, J. Cottam, G.V. Brown, F.S. Porter, and everyone working for Astro-E2/XRS at NASA/Goddard Space Flight Center, and University of Wisconsin. We also would like to thank all our members of the Astro-E2 mission in Japan. T.F. is supported by the Japan Society for the Promotion of Science (JSPS) Postdoctoral Fellowships.

References

- Ikebe, Y. et al. 1999, *ApJ*, 525, 58
- Inogamov, N.A. & Sunyaev, R.A. 2003, *Astron. Lett.* 29, 791
- Stahle, C.K. et al. 2002, *SPIE*, 4851
- Sunyaev, R.A., Norman, M.L., & Bryan, G.L. 2003, *Astron. Lett.* (astro-ph/0310041)